

Noise-induced chaos-order transitions

Fritz Gassmann

Paul Scherrer Institute, General Energy Research, CH-5232 Villigen, Switzerland

(Received 12 September 1996)

Numerical simulations of the Lorenzian water wheel have been used to investigate the influence of stochastic noise on the lifetimes of chaotic transients. Whereas, in one region of parameter space no noise dependency could be detected, a shortening of the lifetimes of more than four decades was found in another region. This large effect was produced by a significant modification of the attraction basin of a quasistable stationary state rather than by affecting the chaotic orbits before the chaos-order transitions occurred. This novel phenomenon of noise-induced chaos-order transitions is not related to stochastic resonance or other noise-induced effects. [S1063-651X(97)06902-X]

PACS number(s): 05.40.+j, 05.45.+b

Complex systems often show ordered stationary or periodic states after a shorter or longer chaotic transient when initialized at random. As stochastic environmental or internal noise is always present in natural systems, the combined effect of chaos and stochastic noise determining the time needed for a system to “find” an ordered state is of interest.

Up to now, much work has been devoted to the investigation of noise-induced transitions from a given stationary state over a barrier to another stationary state. Special attention was given to equilibrium systems governed by an energy potential depending only on one or several space coordinates where a surrounding medium supplies the energy to cross this barrier, and, at the same time, exerts a drag on the system removing energy. Kramers [1] modeled this process by a Langevin equation in his pioneering paper in 1940 and created a branch of theoretical physics still giving new results [2]. Analytical expressions for the transition rate can be used to describe chemical reaction rates, the noise amplitude being defined by temperature.

More recently, theoretical and experimental studies dealt with noise-induced escape from basins of different types of attractors of dissipative, nonlinear dynamical systems far from equilibrium in contrast to the above-mentioned escape from a minimum in the potential energy. For Josephson junctions [3] and for the logistic map [4], the mean escape time was found to decrease with increasing noise amplitude according to an Arrhenius law based on a minimum escape energy. Especially for noise-free chaotic systems in a post-crisis situation, Sommerer, Ott, and Grebogi [5] derived a scaling law for the characteristic times applicable to three types of crises resulting in attractor destruction, attractor enlargement or attractor merging. Further, they generalized this scaling law to precrisis situations where the addition of noise causes the same type of behavior as shown by the noise-free systems in the postcrisis situation. This phenomenon of noise-induced crisis and the applicability of the general scaling law was demonstrated with a magnetoelastic ribbon [6] displaying noise-induced intermittent bursts (attractor enlargement) and with simulations of a Duffing oscillator orbiting intermittently between two symmetric wells [5] (attractor merging). Interestingly, no physical examples seem to be reported for the third type of crisis (attractor destruction leading to transient chaos), where chaos abruptly ceases giv-

ing rise to ordered behavior. Also, with a Duffing oscillator, but in a postcrisis situation, Franaszek and Fronzoni [7] investigated the effect of small noise on the chaos-chaos transitions (“multitransient chaos”) between two asymmetric wells. The times the trajectory spends in one of the two regions were found to be strongly noise dependent. Fedchenia *et al.* [8] observed with analog electronic and computer simulations the emergence of chaotic behavior when periodic attractors in the Lorenz model were disturbed by noise, a phenomenon termed noise-induced chaos.

In contrast to all the above-mentioned investigations, we are interested here in noise dependency of transitions from chaos to ordered (steady, stationary, or periodic) states for postcrisis situations. Franaszek [9] showed for the logistic map and the Hénon map that chaotic evolution may be elongated by a maximum of about 20% when small-amplitude noise is added and shortened with noise of larger amplitude. For the logistic map, a growth parameter of 4.0001 was chosen allowing trajectories to escape to $-\infty$, regarded as an attracting point. However, Blackburn, Grønbech-Jensen, and Smith [10] found no noise dependency for a mathematical pendulum with its point of suspension subjected to a harmonic vertical displacement, either in simulations or experimentally with an electronic analog. Numerical simulations of a parametrically damped pendulum also gave the same null effect. The authors [10] explain this absence of noise dependency with “the specific type of superposition that exists for the attractor basins and the strange attractor remnant,” leading to basins of attraction for the three investigated periodic states “composed chiefly of points randomly peppered over the $(\theta, d\theta/dt)$ plane, together with some rather faint structural features” (θ is the angular coordinate).

After Grebogi, Ott, and Yorke [11], higher-dimensional systems tend to show more persistent chaotic transients over a more extended range of parameter space, indicated by larger values of the respective critical exponents. So, also noise dependency of transient lifetimes might be better observable in systems with considerably higher dimensions as those mentioned above. However, recent investigations by Lai [12] on noise dependency of chaos lifetime for a diffusively coupled logistic map lattice revealed only a negligible effect for this 20-dimensional spatiotemporal system. Based

on these results, he concludes that “the presence of noise is not advantageous in attempts to reduce the transient lifetime.”

We describe here results based on numerical simulations of a Lorenzian water wheel with 12 buckets and thus 14 phase-space dimensions. Originally, this system was designed by W.V. R. Malkus at MIT [13] as a mechanic analog of the rather abstract Lorenz equations [14] and helped to convince the scientific community that deterministic chaos is a reality in physical systems. We will show that noise effects in this spatiotemporal system strongly depend on the system parameters. At a first point *A* in parameter space, we will confirm the above-cited null effect. At another point *B*, however, we will demonstrate for the first time a noise-induced reduction of the transient lifetime exceeding four decades.

The model system investigated here was inspired by an impressive techno-scientific masterpiece exhibited at the Technorama [15] in Winterthur (Switzerland). This water wheel was used for testing the numerical model based on the following equations approximately describing the real system:

$$\begin{aligned} \dot{\varphi} &= \omega \\ \dot{\omega} &= \frac{\sum_{i=0}^{n-1} \nu_i \sin[\varphi + (2\pi i/n)]}{\tau^2} - \frac{\omega}{\tau_2} + \sigma \xi \\ \dot{\nu}_i &= \frac{\delta_i}{\tau_0} - \frac{\nu_i}{\tau_1}, \quad 0 \leq \nu_i \leq 1 \end{aligned} \quad (1)$$

The system consists of n (here $n=12$) buckets spaced equally around the rim of a wheel rotating around a horizontal axis. The top bucket fills when passing under the faucet ($\delta_i=1$ if bucket i is positioned below the faucet and $\delta_i=0$ elsewhere) that delivers water at a steady rate. The buckets leak steadily and a friction proportional to angular velocity ω dissipates energy. One arbitrarily chosen bucket defines the angular position φ and ν_i is the water content in bucket i normalized to 1 (0=empty, 1=full). Key parameters of the system are the time constants τ_0 , τ_1 , and τ_2 signifying the time for an empty bucket to be filled (without drain), the time for a full one to get empty (without inflow), and the friction time constant, respectively. The latter is set to 1.8 s throughout this work. A last parameter $1/\tau^2$ is the maximum angular acceleration exerted from a single full bucket (friction set to zero) and disappears when time is normalized to τ . As τ is set to 1 s for this study, Eq. (1) can be regarded as a dimensionless normalized form. Because of the direct relevance for the mechanic system in Winterthur, we prefer to give the results with physical units.

Noise is coupled to the system as an additive torque noise, according to Blackburn, Grønbech-Jensen, and Smith [10]. σ stands for the amplitude of noise and ξ are numbers from a pseudorandom generator with homogeneous distribution on the interval $[-1,1]$ as used by Franaszek [9]. A new random number is used for every time step Δt set to 0.2 s if not stated otherwise. Several numerical simplifications not affecting our main results were used to save computer time.

Analytical treatment of our model system is rather limited, though some approximations are possible and useful.

So, the stationary states (constant angular velocity ω_s) can be obtained by distributing the water content of the buckets continuously over the wheel's rim:

$$\begin{aligned} \omega_s &= \pm \Theta(\vartheta) \sqrt{\frac{\tau_2 n}{\tau^2 \tau_1}} \\ \Theta(\vartheta) &\equiv \left(\frac{2\pi\vartheta - \sin(2\pi\vartheta)}{2\pi} \right)^{1/2}, \\ \vartheta = \frac{\tau_1}{n\tau_0} < 1, \quad \nu_{\max,s} = \frac{2\pi}{n} \frac{1}{\omega_s \tau_0} < 1, \\ \vartheta_{F1} = 1, \quad \nu_{\max,s} = 1, \quad \frac{\tau_1}{n\tau_0} \geq 1, \\ \vartheta_{F2} = \frac{\omega_s \tau_1}{2\pi} < 1, \quad \nu_{\max,s} = 1, \\ \vartheta_T = 0, \quad \nu_{\max,s} = 0, \quad \tau_1 \leq \tau_0. \end{aligned} \quad (2)$$

$\vartheta \leq 1$ is the relative part of the rim with nonempty buckets or the fraction of time a single bucket contains water. Three types of stable stationary solutions exist depending on the maximum water content $\nu_{\max,s}$ during the filling process: the trivial solution with $\nu_{\max,s}=0$, the intermediate solution to be discussed in more detail with $0 < \nu_{\max,s} < 1$, and two overflow solutions *F1* and *F2* with $\nu_{\max,s}=1$. In the framework of the theory of dissipative systems established by Prigogine [16], the two limits are termed “thermodynamic branch” and “flux branch,” respectively. Stable flux solutions lie outside the parameter range considered in this study: *F1* exists for $\tau_1 \geq n\tau_0$ and *F2* exists in a small portion of parameter space at $\tau_1 < 8\pi^2 \tau^2 / (n\tau_2) \approx 3.66$. To investigate stability of the intermediate solution, we use the continuous model together with the following wave ansatz for the filling density $\nu(\varphi', t)$:

$$\begin{aligned} \nu(\varphi', t) &= \begin{cases} \nu_{\max,s} \left(1 - \frac{\varphi'}{2\pi\vartheta} \right) \\ + \varepsilon \sin\{a(\omega_s t - \varphi')\}, & \varphi' \leq 2\pi\vartheta \\ 0, & \varphi' > 2\pi\vartheta \end{cases} \\ \omega(t) &= \omega_s - \varepsilon \frac{\omega_s}{\nu_{\max,s}} \sin(a\omega_s t). \end{aligned} \quad (3)$$

The independent variable φ' is the angular position of a point on the rim measured from the top of the wheel. The amplitude ε of the top filling density $\nu(0, t)$ is assumed to be small enough to allow terms proportional to ε^2 to be neglected. The system will begin to oscillate at a critical frequency $a\omega_s$ giving the fastest growing ε . Inserting Eq. (3) into the continuous form (integral instead of sum) of Eq. (1) yields the dynamical evolution for ε :

$$\begin{aligned} \dot{\varepsilon} \sin(a\omega_s t) &= \varepsilon \left\{ -a\omega_s \cos(a\omega_s t) - \frac{1}{\tau_2} \sin(a\omega_s t) \right. \\ &\quad \left. - \frac{1}{\tau_2} f(a, \vartheta, t) \right\} \end{aligned} \quad (4)$$

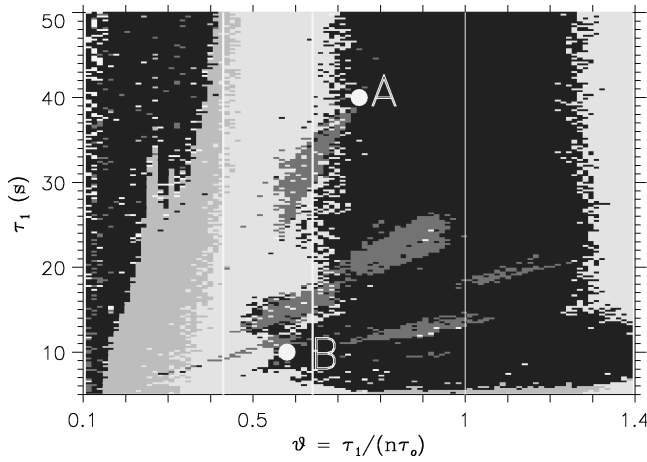


FIG. 1. Solution types on the ϑ - τ_1 plane for $\tau_2=1.8$ s and $n=12$ without noise. Detected states are stationary (light gray), rolling (gray), pendulum (dark gray), and other states with short period (white). The area with no detected short-periodic states (black) contains chaos, states with long period and chaotic supertransients. The vertical lines are stability limits according to Eqs. (2)–(6). A and B are the two points to be investigated here: at A, no noise dependency was found and at B, very large noise dependency was found.

$$f(a, \vartheta, t) \equiv \frac{f_1 \sin a' + f_2 \cos a'}{1 - \frac{\sin(2\pi\vartheta)}{2\pi\vartheta}}$$

$$a' \equiv a\omega_s t$$

$$f_1(a, \vartheta) \equiv \frac{1 - \cos\{(a+1)2\pi\vartheta\}}{2(a+1)} - \frac{1 - \cos\{(a-1)2\pi\vartheta\}}{2(a-1)}$$

$$f_2(a, \vartheta) \equiv \frac{\sin\{(a+1)2\pi\vartheta\}}{2(a+1)} - \frac{\sin\{(a-1)2\pi\vartheta\}}{2(a-1)}.$$

The growth rate for ε averaged over half a period $\pi/a\omega_s$ can be shown to be equal to the instantaneous growth rate at time t_1 defined by $a\omega_s t_1 = \pi/2$. For this time, point Eq. (4) reads

$$\dot{\varepsilon} = \frac{\varepsilon}{\tau_2} \{-1 + f(a, \vartheta)\},$$

$$f(a, \vartheta) \equiv \frac{1/2}{1 - \sin(2\pi\vartheta)/2\pi\vartheta} \left\{ \frac{1 - \cos[(a-1)2\pi\vartheta]}{a-1} - \frac{1 - \cos[(a+1)2\pi\vartheta]}{a+1} \right\}. \quad (5)$$

The critical frequency $a\omega_s$ and the respective exponent λ are given by

$$\lambda = \frac{1}{\tau_2} \max_a \{-1 + f(a, \vartheta)\}. \quad (6)$$

Numerical evaluation gives stable intermediate stationary solutions ($\lambda < 0$) in the range $\vartheta \approx [0.43, 0.64]$ with critical $a \approx 1.7$.

Figure 1 shows an overview of the types of behavior found with the discrete model according to Eq. (1) without

noise. The results of 100×100 randomly initialized transients of at most 200 000 time steps each are shown. Detected ordered states were the stationary states according to Eq. (2), all symmetrically oscillating pendulum states with different amplitudes, periodic rolling states with variable angular velocity but without changes of sign and other periodic states with periods shorter than 80 s. The latter were defined by the maxima of the autocorrelation of ω exceeding 0.97. Inspection of a number of these states revealed a rich variety of symmetrical and asymmetrical periodic orbits together with a minority of irregular rather than periodic orbits. If none of the above-mentioned ordered states were detected after 200 000 time steps, the asymptotic state at the respective parameter values is either chaotic or has a period longer than 80 s or the chaotic transient exceeds 40 000 s. In spite of the approximate character of the stability analysis and the model simplifications, the stability limits for the stationary solutions according to Eqs. (3)–(6) give good estimates for $\tau_1 \geq 20$ s. The critical value $\vartheta = 1$ for the stable flux solution $F1$ cannot be found by the described method because there is no overlap of the chaotic attractor and the stable $F1$ attractor below $\vartheta \approx 1.22$. Simulations show, however, that stable $F1$ solutions exist also for $1 < \vartheta < 1.22$. In addition, the theoretical values for ω_s according to Eq. (2) differ by less than 12% from the simulated values in the whole portion of parameter space shown in Fig. 1.

Point A ($\vartheta = 0.75$, $\tau_1 = 40$ s) is located in the region with transient chaos decaying predominantly to the stationary state, but to a lesser extent also to pendulum states with different amplitudes. Randomly initialized simulations (ω in the range $[-2, 2 \text{ s}^{-1}]$, all 13 other variables in the maximum possible range) with different additive torque noise amplitudes were performed. The exponential distribution of the duration of the chaotic transients reported by several authors [9–11] according to

$$N(t) = N_0 e^{-t / (\ln 2) T} \quad (7)$$

could be confirmed. Here, T is the time needed for half of the $N_0 = 10^4$ transients simulated for each noise level to find a stationary state (transitions to other detected periodic states were correctly taken into account). It could be shown with a consistency test based on the number of transitions in different time intervals that the deviations from Eq. (7) can be explained by statistical fluctuations for all but two points represented in Fig. 2. These two points with poor consistency represent about 20% of the ensemble of points for noise amplitudes below $4 \times 10^{-3} \text{ s}^{-2}$. In contrast, their statistical frequency should be below 4%. The occurrence of ordered states with long periods (> 80 s) would give erroneous results with exaggerated chaos lifetimes and might be a reason for the observed poor consistency. Figure 2 shows a mean transient half lifetime $T = 432 \pm 39$ h for the calculated “supertransients” (a term introduced by Lai [12] for very long transients) being independent of noise with amplitudes covering a range of more than three decades. This result is consistent with the above-mentioned null effect reported by Blackburn, Grønbech-Jensen, and Smith [10]. The increase of T for large noise amplitudes is due to orbits escaping from the stationary states less than 800 s after capture. Such back-transitions from order to chaos can be described in principle

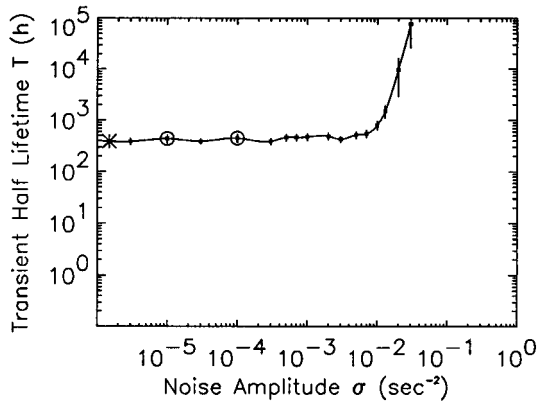


FIG. 2. Time needed for half of 10^4 chaotic transients to find a stationary state for different noise amplitudes σ at point A ($\vartheta=0.75$, $\tau_1=40$ s). Error bars indicate \pm twice the standard deviation; circles indicate points with poor consistency (see text); the asterisk indicates noiseless transients.

by a combination of the Arrhenius law and the dissipation-fluctuation theorem [$\sigma^2 \sim (\text{temperature})$] giving [3]

$$T' \sim e^{\Delta E/\sigma^2}, \quad (8)$$

where T' is the average time for escape from the basin of a quasistable periodic attractor caused by noise of amplitude σ and ΔE is the minimum escape energy [4].

In the vicinity of point A, a scaling law as described by Grebogi, Ott, and Yorke [11] for low-dimensional maps and by Blackburn, Smith, and Edmundson [17] for a parametrically damped pendulum, could be found also for the noise-free Lorenzian water wheel. The mean half lifetime T of transients from chaos to one of the two stationary states depends upon the system parameter ϑ via

$$T \sim |\vartheta - \vartheta_c|^{-\gamma}, \quad (9)$$

where ϑ_c denotes a critical value of ϑ , and γ is the critical exponent. Figure 3 shows Eq. (9) being satisfied over roughly one decade of $|\vartheta - \vartheta_c|$ and over four decades of T , suggesting a critical exponent $\gamma \approx 3.9$. These results support the conjecture stated by Grebogi, Ott, and Yorke [11] that γ tends to be larger for more-dimensional systems, being 0.5 for one-dimensional maps with a quadratic maximum, and $1, \dots, 2$ for two-dimensional maps. For the three-dimensional parametrically damped pendulum, Blackburn, Smith, and Edmundson [17] found $\gamma \approx 1$. What they pointed out for the pendulum, namely that transient chaos does not arise out of a boundary crisis, seems to be true also for the Lorenzian water wheel. Rather, the stable attractors for the stationary states are born at ϑ_c near the chaotic attractor and their basins partly overlap with it. However, we find it confusing to speak about a “destroyed,” “remnant,” or “ghost” strange attractor [17] after the birth of the stable attractor at ϑ_c . Rather, the dynamical structure called “chaotic or strange attractor” changes smoothly and continuously over a certain range in parameter space containing the critical value ϑ_c . There, basins of quasistable attractors begin to grow and overlap with increasing portions of the chaotic attractor, thus reducing chaos lifetime according to Eq. (9).

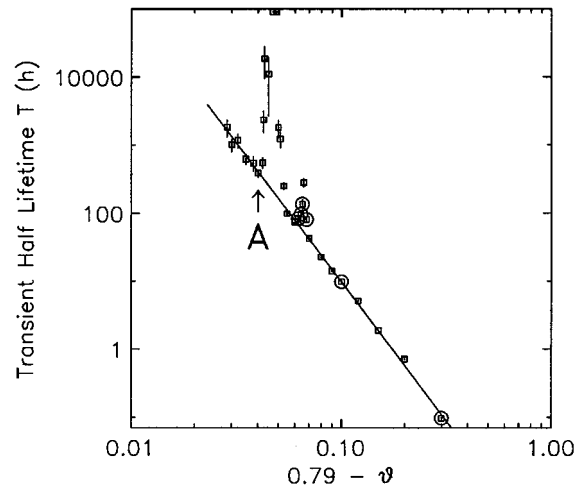


FIG. 3. Average transition times from chaos to a stationary state for different ϑ and for zero noise. Each dot was obtained by an averaging of 10^4 transients starting at randomly chosen points in phase space. Circles indicate very poor consistency (see text); points at upper figure boundary denote absence of transitions to stationary states; error bars indicate \pm twice the standard deviation; straight line corresponds to Eq. (9) with critical exponent $\gamma \approx 3.9$; peaks result from transitions to pendulum states.

The situation is reminiscent of a labyrinth not destroyed by an additional door to the outside, but only made a little easier to escape from. The peaks in Fig. 3 arise from narrow tongues of concurring pendulum states as shown in Fig. 1, reducing transition probabilities to the stationary states. Further, some points show very poor consistencies with Eq. (7). Only less than 1 in 10^5 points having such low consistencies could be explained by statistical fluctuations. Inspection of probabilities for transitions to the stationary states in different time intervals revealed maxima for some intervals and often a decay to low values for long times. Undetected long periodic orbits might offer an explanation for this strange effect.

Point B ($\vartheta=0.58$, $\tau_1=10$ s) is located in a region of parameter space with complicated structure, where different short periodic stable orbits coexist with the stationary states and chaotic supertransients. A scaling law for the noise-free system according to Eq. (9) could not be found due to erratic behavior of $T(\vartheta)$. Repetition of calculations leading to Fig. 1, but this time with high additive torque noise, showed a dramatically changed region around point B, indicating noise dependency. Analogously to Fig. 2, Fig. 4 was calculated showing very important noise dependency of transition times from chaos to the stationary states. Three noise regimes with different behavior of our model system were found, the most surprising being regime B_3 where transition times are reduced by more than three decades. All calculations gave distributions of transition times consistent with Eq. (7) after discarding the first 30 s. Deleting a small time interval after initialization was necessary to eliminate transients that reached the stationary state quickly (typically within less than 10 s), without any indication of chaos, an observation made also by Blackburn, Smith, and Edmundson [17] with the parametrically damped pendulum. For the 24 points with $\sigma \leq 0.6$ s $^{-2}$, an average of 411 ± 25 transients out of 10 000

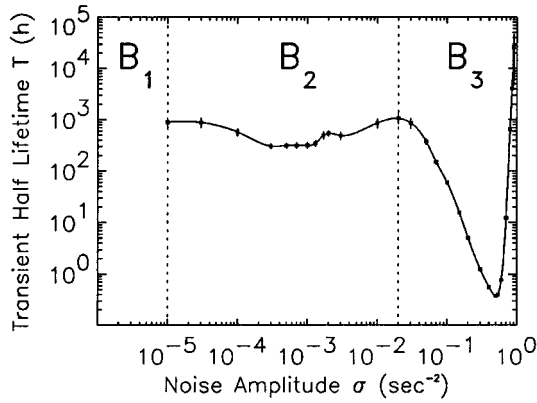


FIG. 4. Time needed for half of 10^4 chaotic transients to find a stationary state for different noise amplitudes σ at point B ($\vartheta=0.58$, $\tau_1=10$ s). Error bars indicate \pm twice the standard deviation; noise regimes with different behavior are numbered B_1 – B_3 .

(i.e., 4.11%) were affected. The basins for the stationary states with $\omega \approx \pm 1.05$ s $^{-1}$ occupy, therefore, 4.11% of phase-space volume (for ω confined to the range ± 2 s $^{-1}$) homogeneously filled with initial conditions. The probability for one single randomly chosen variable to lie within these large basins is 79.6% on the average (i.e., $0.796^{14}=0.041$).

Regime B_1 with very small noise ($\sigma < 10^{-5}$ s $^{-2}$) displays noise-induced chaos as observed, for example, by Fedchenia *et al.* [8] with the Lorenz system based on analog and digital simulations. Without noise or with very weak noise, randomly initialized transients get trapped relatively quickly (typically within less than 10 h) by different ordered states with very long periods of the order of 10^3 s. Several of these complicated periodic orbits could be detected using a two-dimensional plane in phase space to be discussed below. One transient with period 2583.0 s was found that almost resisted a noise amplitude of 10^{-6} s $^{-2}$ (eight full periods were completed before the orbit turned chaotic; see Fig. 7). We consider these very long periodic orbits not as mere artifacts only (they surely cannot be observed with real water wheels because they depend on the integration time step Δt that has to be understood as an additional system parameter), but as properties of the model system being perhaps of more general importance.

Regime B_2 with small noise ($10^{-5} < \sigma < 2 \times 10^{-2}$ s $^{-2}$) is characterized by irregular and so far unexplained variations of transition times by a factor of three and might be worth being investigated in more detail. Sensitivity studies with reduced time steps showed important increases of transition times. With $\Delta t=0.1$ s, roughly constant values around 4000 h were calculated and with $\Delta t=0.03$ s, no transitions to the stationary states could be found in this low-noise region. The integration time step has thus to be regarded as an additional system parameter also in this region.

Regime B_3 with large noise ($\sigma > 0.02$ s $^{-2}$) has been most carefully investigated in this study. To our knowledge, such dramatic shortening of chaotic transients by noise is reported here for the first time. Inspection of many transitions from chaos to one of the two symmetric stationary states with noise amplitude $\sigma=0.5$ s $^{-2}$ showed very clearly defined and abrupt phase changes always preceded by a characteristic ‘‘swing into the other direction’’ to a maximum of $|\omega| \approx 2$

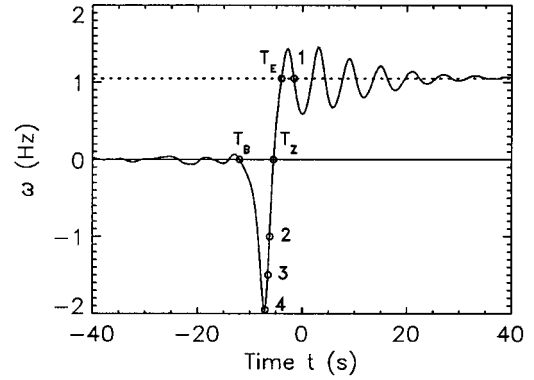


FIG. 5. Average over 1367 transients from chaos to the stationary state with positive angular velocity $\omega=1.05$ s $^{-1}$ in the presence of noise with amplitude $\sigma=0.5$ s $^{-2}$. Transition roughly begins at relative time $T_B \approx -12$ s and ends at $T_E \approx -4$ s. T_Z indicates the last zero crossing before capture into the stationary state; numbers 1–4 refer to Fig. 6.

s $^{-1}$. This regularity allowed a superposition of many transitions (using the well defined last zero crossing point T_Z for adjustment) giving an average transition as shown in Fig. 5. Before transitions begin at $T_B \approx -12$ s, the different chaotic and noisy transients average to almost zero. After the above-mentioned characteristic swing, a typical damped oscillation around the stationary state follows that belongs to the stable attractor and is not part of the transition taking place in only about 8 s. To investigate system behavior near T_B , a two-dimensional plane Π was defined in the 14-dimensional phase space containing T_B and two arbitrarily chosen symmetrical points on the chaotic attractor. By choosing appropriate coordinates, the origin of Π coincides with T_B . Figure 6 clearly shows the fractal nature of the attraction basin for the stationary states on this plane. The time interval of 100 s chosen for acceptance of a starting point to lie within the

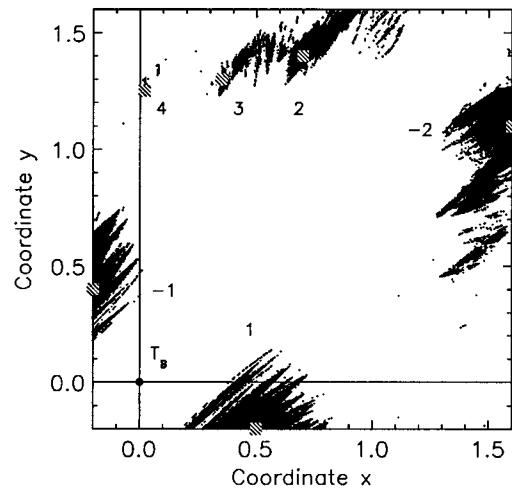


FIG. 6. Part of the attraction basin for the two stationary states on plane Π without noise as found by scanning of Π with 500×500 points. The origin corresponds to point T_B in Fig. 5; positive numbers indicate approximate starting points as indicated in Fig. 5; negative numbers refer to the symmetric stationary state with $\omega = -1.05$ s $^{-1}$.

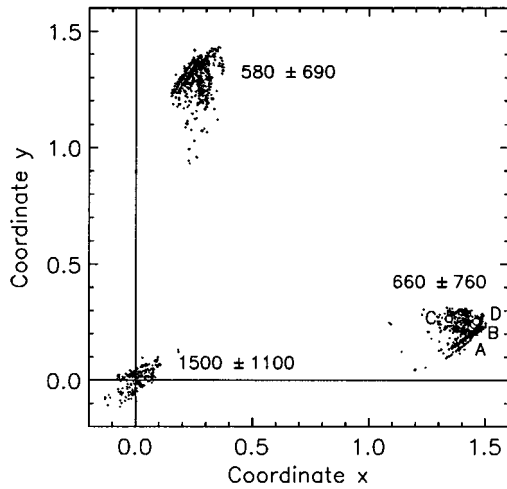


FIG. 7. Points of the chaotic attractor with distances smaller than $d=0.05$ from plane Π for noise amplitude $\sigma=0.03 \text{ s}^{-2}$. A periodic orbit stable with very small noise only ($\sigma < 10^{-6} \text{ s}^{-2}$) and period 2583.0 s is indicated by points A–D. The metrics chosen for Π and also for calculating distances is $g^i = (g^\varphi, g^\omega, g^{\nu_1}, \dots, g^{\nu_{12}}) = (1/2\pi, 1/4, 1, \dots, 1)$. The numbers indicate average recurrence times (in seconds) with standard deviations for the three regions around the three points chosen to define Π .

basin of one of the two stable attractors, revealed not to be critical for two reasons. First, transition times for trapped trajectories starting on the portion of Π shown are below 4 s as indicated in Fig. 6. Second, the lifetime of chaotic transients is well above 100 s as soon as a trajectory starting on Π is on the chaotic attractor. The attraction basin is thus astonishingly well defined as pointed out already by Blackburn, Smith, and Edmundson [17] for the parametrically damped pendulum. Remarkably, the origin of Π chosen as the average beginning point of transitions does not belong to the attraction basin, implying that the average transient shown in Fig. 5 does not exist (being a mere product of the averaging process).

To determine points of the chaotic attractor nearest to Π , a somewhat arbitrary threshold distance d has to be defined. The value of $d=0.05$ according to the metrics g^i indicated in Fig. 7 resulted from a trial and error procedure and can be supported by the following reasoning: the dominant process for determining distances between successive points in phase space is $\Delta v_i / \Delta t \approx -1/\tau_1$ for 11 buckets giving steps of at least $11^{1/2} \times 0.2/10 \approx 0.07$. So, many points would get lost with $d \ll 0.07$. Comparison of Figs. 6 and 7 shows a very small overlapping zone near coordinates (0.38/1.3), which can explain the observed time that it takes for half of the chaotic transients to find the stationary state. Assuming that one of the 2504 points of the respective cloud in Fig. 7 with an average recurrence time of 580 s is located in the basin of the stable attractors, $T \approx \ln(2) \times 2504 \times 580 \text{ s} \approx 280 \text{ h}$. This is of the order of the observed 400 h.

Surprisingly, the three clouds of points in Fig. 7 were almost unaffected by noise, merely slightly smeared out with large noise amplitudes. The increased overlap between the chaotic attractor and the basin of the stable attractors according to Fig. 6 produced by this noise effect could explain a reduction of chaos lifetime by a small factor only, by far

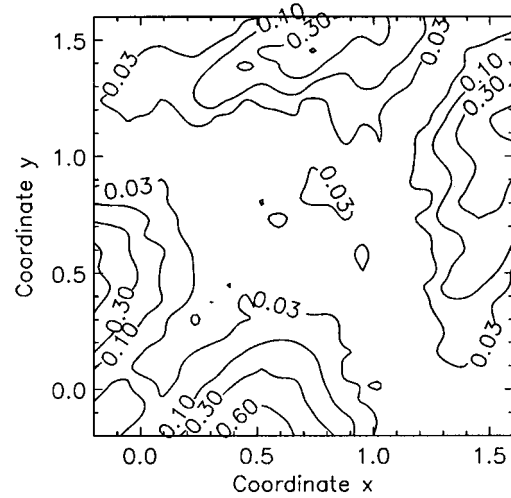


FIG. 8. Probability of transitions to a stationary state within less than 40 s in the presence of torque noise with amplitude $\sigma=0.5 \text{ s}^{-2}$. Isolines for probability 0.3 roughly indicate the attraction basin without noise as shown in Fig. 6. Probabilities are based on 1000 transients calculated in each point of a 25×25 grid.

smaller than the observed three orders of magnitude. This discrepancy could be eliminated by calculating a generalized basin for the stable attractors in the presence of noise. Figure 8 shows transition probabilities of 3–10 % in the three chaotic attractor regions shown in Fig. 7. By taking into account recurrence times of $T_i = 950 \pm 940$, 650 ± 700 , and $650 \pm 660 \text{ s}$ for the three clouds (from left to right) with noise amplitude $\sigma=0.5 \text{ s}^{-2}$ and probabilities $p_i = 0.03$, 0.1, and 0.05, respectively, an upper limit of T can be estimated by

$$T < \frac{\ln 2}{p}, \quad p = \sum_{i=1}^3 \frac{p_i}{T_i}, \quad (10)$$

giving a correct order of $T < 0.73 \text{ h}$ (the simulated T is 0.38 h, see Fig. 4). Equation (10) gives an upper bound for T because of other possible transients to the stable attractor not “touching” Π . Further, Eq. (10) gives an explanation for the validity of the exponential transient length distribution according to Eq. (7) in the presence of large noise; the constant transition probability per time unit leading to Eq. (7) is equal to the quotient of transition probabilities smoothly distributed in phase space and recurrence times for trajectories on the chaotic attractor to such probabilistic entry points to the stable attractors.

For lower noise levels, the validity of Eq. (7) seems to rely on a different physical process, namely, an overlapping of parts of the chaotic attractor with the basin of the stable attractors. In this situation, the transition probability might be defined by a geometrical fraction of overlap region and a suitably defined characteristic volume in phase space circumscribing the chaotic attractor, as proposed also vaguely by Blackburn, Smith, and Edmundson [17]. The random-walk-like behavior of trajectories on the chaotic attractor (due to the “butterfly effect”) would then produce the constant transition probability per unit of time. For a rather compact structure of the basin of the stable attractor similar to the one shown in Fig. 6, a small noise dependency could arise from a slightly smeared out chaotic attractor, leading to increased

or decreased transition times as observed in regime B_2 . For a highly *dispersed attraction basin* as described by Blackburn *et al.* [10,17], however, small displacements of chaotic trajectories due to noise cannot affect the probability of encountering parts of the basin. The situation could be illustrated by a rather strange variant of golf with a big number of invisible holes distributed regularly over the area. The probability of winning would not be affected by a storm or by a player being blind or drunk. Also, high noise amplitudes converting the attraction basin into a smooth probability field might not affect transient lifetimes for systems with a dispersed attraction basin and so lead to the above-cited null effect [10].

The reported noise-induced shortening of chaotic transients by roughly three decades could be increased by decreasing the integration time step Δt from 0.2 s to 0.1 and 0.03 s. The sharp minimum of T fell below 0.35 h to 0.16 and 0.12 h, respectively. Combined with the above stated increased transition times for small noise amplitudes (regime B_2) when time steps are reduced, the noise effect appears to exceed four decades. As reduced time steps tend to increase the effect of noise-induced shortening of chaotic transients, we expect the phenomenon presented here to be a physical reality that will be encountered also with different (mechanic, electronic, chemical, perhaps biological) real-world systems.

At very large noise amplitudes ($\sigma > 0.5 \text{ s}^{-2}$), a sharp increase of mean transition times to the stationary states arises from noise-induced transitions from the quasistable states back to the chaotic attractor (i.e., noise-induced chaos [8]), and can be described [3] in principle by an Arrhenius relation according to Eq. (8), as stated above.

The noise-induced chaos-order transitions described here do not seem to be variants of other noise phenomena discovered over the last decade. Stochastic resonance (SR) in par-

ticular, originally discovered and developed by Benzi, Sutera, and others [18,19], has attracted increasing attention in theoretical studies and applications [20,21]. However, some recently discovered noise effects are clearly not related to any kind of frequency matching (e.g., noise-induced stabilization [22]) but are sometimes nevertheless called SR by their authors (e.g., noise-induced threshold crossings [23], noise-induced oscillations [24]). All these noise effects differ substantially from the noise-catalyzed spontaneous emergence of ordered structures out of chaos that are described here. Further, its mechanism is not a noise-induced escape from a chaotic attractor and, therefore, might not be described with the above-mentioned general scaling law [5] applicable to noisy pre-crisis situations. Rather, noise transforms the basin of a stable order-attractor with fractal boundaries into a generalized smooth probabilistic basin filling large portions of phase space that overlaps significantly with the (practically unaffected) chaotic attractor. We conjecture, therefore, that the noise effect might not be described by a noise-induced probability of escape from the chaotic attractor as in Ref. [5], but rather by a noise-induced *trapping probability* of the stable order attractor. Finally, the effect described here is, at least for our model system, independent of the way noise is coupled to the system. Instead of a coupling to the variable ω as torque noise, coupling to the parameter τ_0 simulating a noisy water supply gives qualitatively the same results.

The general characterization of systems and locations in parameter space showing the large noise effect reported here is at the moment an open question. Potential fields of interest might be biological evolution theory, cognition physiology, economy, ecology, climate dynamics, and other research areas dealing with complex multistable systems subjected to high noise levels.

-
- [1] H. A. Kramers, *Physica* **7**, 284 (1940).
 [2] P. Talkner, P. Hänggi, *New Trends in Kramers' Reaction Rate Theory* (Kluwer, Dordrecht, 1994).
 [3] P. Grassberger, *J. Phys. A* **22**, 3283 (1989).
 [4] P. D. Beale, *Phys. Rev. A* **40**, 3998 (1989).
 [5] J. C. Sommerer, E. Ott, and C. Grebogi, *Phys. Rev. A* **43**, 1754 (1991).
 [6] J. C. Sommerer, *Phys. Lett. A* **176**, 85 (1993).
 [7] M. Franaszek and L. Fronzoni, *Phys. Rev. E* **49**, 3888 (1994).
 [8] I. I. Fedchenia, R. Mannella, P. V. E. McClintock, N. D. Stein, and N. G. Stocks, *Phys. Rev. A* **46**, 1769 (1992).
 [9] M. Franaszek, *Phys. Rev. A* **44**, 4065 (1991).
 [10] J. A. Blackburn, N. Grönbech-Jensen, and H. J. T. Smith, *Phys. Rev. Lett.* **74**, 908 (1995).
 [11] C. Grebogi, E. Ott, and J. A. Yorke, *Phys. Rev. Lett.* **57**, 1284 (1986).
 [12] Y. C. Lai, *Phys. Lett. A* **200**, 418 (1995).
 [13] S. H. Strogatz, *Nonlinear Dynamics and Chaos* (Addison-Wesley, Reading, MA, 1994).
 [14] E. N. Lorenz, *J. Atmos. Sci.* **20**, 130 (1963).
 [15] Pro Technorama No. 4 (Winterthur, Switzerland, 1994).
 [16] I. Prigogine, *Introduction to Thermodynamics of Irreversible Processes* (Wiley, New York, 1961).
 [17] J. A. Blackburn, H. J. T. Smith, and D. E. Edmundson, *Phys. Rev. A* **45**, 593 (1992).
 [18] A. Sutera, *Quart. J. Roy. Meteorol. Soc.* **107**, 137 (1981).
 [19] R. Benzi, A. Sutera, and A. Vulpiani, *J. Phys. A* **14**, 453 (1981).
 [20] P. Jung, *Phys. Rep.* **234**, 175 (1993).
 [21] M. I. Dykman, D. G. Luchinsky, R. Mannella, P. V. E. McClintock, N. D. Stein, and N. G. Stocks, *Nuovo Cimento D* **17**, 661 (1995).
 [22] R. Wackerbauer, *Phys. Rev. E* **52**, 4745 (1995).
 [23] L. Gammaitoni, *Phys. Rev. E* **52**, 4691 (1995).
 [24] G. Hu, T. Ditzinger, C. Z. Ning, and H. Haken, *Phys. Rev. Lett.* **71**, 807 (1993).